

Critical scaling of jammed system after quench of temperature

Michio Otsuki¹ and Hisao Hayakawa²

¹ *Department of Physics and Mathematics, Aoyama Gakuin University,
5-10-1 Fuchinobe, Sagami-hara, Kanagawa 229-8558, Japan*

² *Yukawa Institute for Theoretical Physics, Kyoto University,
Kitashirakawa-oiwake-cho, Sakyo-ku, Kyoto 606-8502, Japan*

Critical behavior of soft repulsive particles after quench of temperature near the jamming transition is numerically investigated. It is found that the plateau of the mean square displacement of tracer particles and the pressure satisfy critical scaling laws. The critical density for the jamming transition depends on the protocol to prepare the system, while the values of the critical exponents which are consistent with the prediction of a phenomenology are independent of the protocol.

PACS numbers: 64.70.Q, 64.70.kj, 61.43.-j, 05.70.Jk

I. INTRODUCTION

The jamming transition has attracted many physicists since Liu and Nagel indicated its similarity to the glass transition [1]. In naive sense, the glass transition is characterized by a divergence of time scale on a temperature-density plane [2–4], while the jamming transition is an athermal transition on a density-load plane as the emergence of rigidity for materials such as granular materials, forms, and colloidal suspensions [5–7]. For frictionless particles, it is known that the pressure, the elastic modulus, and the characteristic frequency for the soft mode continuously emerge above a jamming transition point, while the coordination number changes discontinuously at the point [8–11].

The jamming transition was discussed mainly on the axis of the density without any load and temperature in some pioneer works [8–11]. It is instructive, however, that critical properties have been clarified when we look at the behavior of the jamming on the density-load plane in the zero load limit. For instance, critical scaling laws for the rheological transition, similar to those in continuous phase transitions, have been observed for sheared frictionless systems [12–21], while the discontinuous transition and the hysteresis loop are observed in the pressure and the shear stress for sheared frictional granular materials [22, 23].

Coming back to the original idea in Ref. [1], we can also discuss the jamming transition on the density-temperature plane, i.e. without any load. This approach has an advantage to clarify the relationship between the glass transition [2–4] and the jamming transition [5–7], because the glass transition is originally defined only on the temperature-density plane. So far the behavior on the density-temperature plane in the zero temperature limit has been studied by some researchers, but the situation is still confusing. Indeed, some indicated that the critical fraction ϕ_G for the divergence of the relaxation time in the zero temperature limit is identical to the critical point ϕ_J for the jamming transition of the athermal materials [24, 25], while the others suggested that two transition points are different [26–30]. It is re-

markable that Berthier and Witten have numerically confirmed from their simulation for soft repulsive particles at low temperature that (i) the relaxation time around the glass transition point ϕ_G satisfies a scaling relation, and (ii) ϕ_G is lower than that for the jamming point ϕ_J [29, 30]. It is also noticed that the separation between ϕ_G and ϕ_J is clearly demonstrated from a simulation for sheared soft spheres in the zero temperature and zero shear limits [31].

Recently, the critical behavior of repulsive particles on the density-temperature plane near the jamming transition at zero temperature and high density has been studied both numerically and theoretically [32–35]. It is notable that the replica theory gives a prediction on both the critical fraction and the critical exponents [32, 33]. The validity of their prediction for the critical behavior of the pressure, the energy, and the divergence of the first peak of the radial distribution function have numerically verified [32, 33]. However, it is unclear whether the critical exponents are unique because they might depend on the protocol to prepare the system as for the critical density of the jamming transition [36, 37].

In this paper, to clarify critical behavior on the density-temperature plane in the vicinity of the jamming transition point, we numerically investigate the value of plateau (VP) of the mean square displacement (MSD) of tracer particles and the pressure of soft repulsive particles after quench of temperature and demonstrate that the critical exponents for critical scaling laws does not depend on the protocol, while the protocol dependence exists in the critical fraction. We should note that the pressure for soft spheres [33] and MSD for hard spheres [34] have been numerically measured in the previous papers, but this paper is the first report on the numerical study of MSD for soft spheres.

The organization of this paper is as follows. In the next section, we will explain our set up and models. In Sec. III, we show the results of our simulation on the critical behavior for VP and the pressure of the quenched soft particles. In Sec. IV, we will show the jamming transition density depends on the protocol to prepare the system. In Sec. V, we will present scaling laws for the plateau and the pressure, and theoretically determine the

critical exponents. In Sec. VI, we will discuss and conclude our results.

II. SETUP AND MODEL

We study a three dimensional system consists of N soft spherical particles with mass m enclosed in a periodic cube of linear size L . Note that the box size L is fixed for the most cases, but is changed when we will determine the jamming point in Sec. IV. We prevent the system from crystallization by using a 50:50 binary mixture of spheres of diameter ratio 1.4 which is numerically confirmed from the radial distribution function, where sharp peaks characterizing crystallization do not exist [8, 9, 29, 30]. It should be noted that the critical behavior for jamming transition of granular particles is unchanged even for a mono-disperse system or a poly-disperse system with equal number of particles of diameters σ_0 , $0.9\sigma_0$, $0.8\sigma_0$, and $0.7\sigma_0$ [8, 9, 18].

For later convenience, let us use dimensionless quantities scaled by σ_0 for the length, m for the mass, and $\sqrt{m\sigma_0^2/\epsilon}$ for the time, respectively, where we have introduced a characteristic energy scale ϵ . We assume that the interaction between i and j particles is described by a pair wise potential

$$V(r_{ij}) = (1 - r_{ij}/\sigma_{ij})^2 \theta(\sigma_{ij} - r_{ij}), \quad (1)$$

where $\theta(x)$ is the Heaviside step function satisfying $\theta(x) = 1$ for $x \geq 0$ and $\theta(x) = 0$ for otherwise, $r_{ij} = |\mathbf{r}_i - \mathbf{r}_j|$ and $\sigma_{ij} = (\sigma_i + \sigma_j)/2$ with the position \mathbf{r}_i and the diameter σ_i of the particle i .

We start from an equilibrium state at an initial temperature T_I and a volume fraction ϕ . Then, we quench the system directly to a final temperature T_F , and the system subsequently evolves at T_F by the velocity rescaling thermostat. We use the system size $N = 1000$. We have checked the critical exponents do not change when we use $N = 4000$. We adopt the leap-frog algorithm with the time interval $\Delta t = 0.01$. We have verified that the choice of the algorithm does not affect the average values of the pressure and MSD within the numerical accuracy when we use the velocity Verlet algorithm and $\Delta t = 0.001$. We believe that the initial state is sufficiently equilibrated. Indeed, as long as we have checked, MSD exceeds 10 and we could not find any aging effects during the equilibration process. This system has been well studied in the previous papers on the energy, the pressure, and the radial distribution function [32, 33].

III. MEAN SQUARE DISPLACEMENT AND PRESSURE

In this section, we summarize the results of our simulation on MSD and the pressure. Note that the system has a fixed volumed fraction ϕ or a fixed volume in this section.

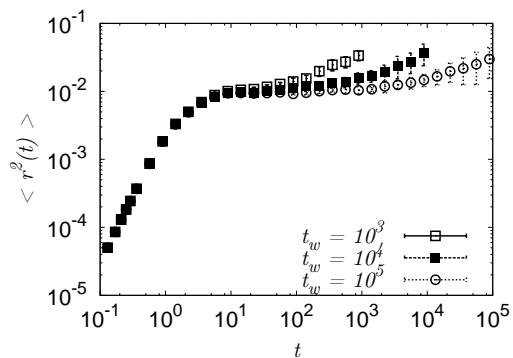


FIG. 1: MSD $\langle r^2(t) \rangle$ as a function of time t for $\phi = 0.7$, $T_I = 10^{-2}$ and $T_F = 10^{-3}$ with $t_w = 10^3, 10^4$, and 10^5 .

First, let us consider the mean square displacement of larger tracer particles at T_F

$$\langle r^2(t) \rangle \equiv \sum_i^{N/2} \frac{\langle |\mathbf{r}_{L,i}(t + t_w) - \mathbf{r}_{L,i}(t_w)|^2 \rangle}{N/2}, \quad (2)$$

where $\mathbf{r}_{L,i}(t + t_w)$ and t_w are the position of the larger particle i and the waiting time, i.e., the time elapsed after the quench, respectively. Here, we ignore the displacement of the smaller particles in order to eliminate the effect of rattlers [9]. The bracket denotes an equilibrium ensemble average over the initial configurations. In Fig. 1, we plot MSD $\langle r^2(t) \rangle$ as a function of the time t with $\phi = 0.7$, $T_I = 10^{-2}$, $T_F = 10^{-3}$ for the waiting time $t_w = 10^3, 10^4$, and 10^5 , where MSD exhibits clear plateaus. The time to escape from the plateau increases as the waiting time t_w increases, which indicates that the system does not reach an equilibrium state within the time window explored in our simulation [38]. However, we should note that VP is independent of the waiting time t_w .

In Fig. 2, we plot MSD as a function of the time t divided by the “thermal” time $\tau_T \equiv 1/\sqrt{T_F}$ for $\phi = 0.62$, $T_I = 10^{-2}$, $t_w = 10^5$ with $T_F = 10^{-4}, 10^{-5}, 10^{-6}$, and 10^{-7} . Thanks to the introduction of the scaled time t/τ_T , MSD for $\phi = 0.62$ converges to a master curve, which indicates that VP is almost independent of the final temperature T_F . For relatively low density case, it is known that the particles behave as a hard sphere liquid, in which the dynamics is independent of the temperature if the time is scaled by the thermal time [29, 30]. This is the reason for the scaling behavior as shown in Fig. 2.

On the contrary, MSD strongly depends on T_F for denser cases. In Fig. 3, we show $\langle r^2(t) \rangle$ scaled by T_F as a function of the time t for $\phi = 0.70$, $T_I = 10^{-2}$, and $t_w = 10^5$ with $T_F = 10^{-4}, 10^{-5}$, and 10^{-6} . MSD $\langle r^2(t) \rangle$ scaled by T_F converges to a master curve, which indicates that VP is proportional to T_F . For this case, a particle is completely trapped within a cage and fluctuates around its equilibrium position. The reason why VP is proportional to T_F can be understood as follows. The energy δE

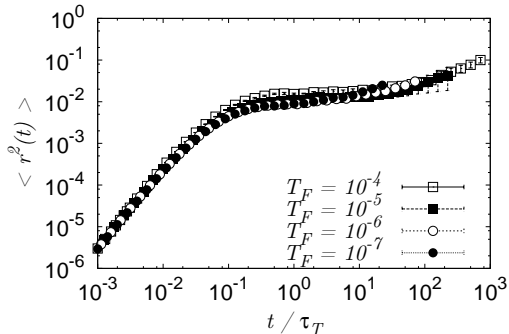


FIG. 2: MSD $\langle r^2(t) \rangle$ as a function of the time t scaled by the thermal time τ_T for $\phi = 0.62$, $T_1 = 10^{-2}$ and $t_w = 10^5$ with $T_F = 10^{-4}, 10^{-5}, 10^{-6}$, and 10^{-7} .

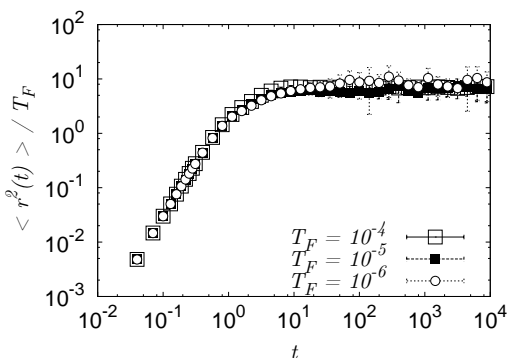


FIG. 3: MSD $\langle r^2(t) \rangle$ scaled by T_F as a function of t for $\phi = 0.70$, $T_1 = 10^{-2}$ and $t_w = 10^5$ with $T_F = 10^{-4}, 10^{-5}$, and 10^{-6} .

due to the fluctuation of its position $\delta\mathbf{r}$ may be approximated as $\delta E \propto |\delta\mathbf{r}|^2$. If we assume that the distribution of $\delta\mathbf{r}$ satisfies $\rho(\delta\mathbf{r}) \propto \exp(-\delta E/T_F)$, $\rho(\delta\mathbf{r})$ depends on through $|\delta\mathbf{r}|^2/T_F$. If we also assume that VP is scaled by the size of the fluctuation $\langle |\delta\mathbf{r}|^2 \rangle$, it is reasonable to obtain the scaling relation as in Fig. 3.

Here, let us introduce m_p as $\langle r^2(t) \rangle$ at $t = \tau_T$. We should note that $\langle r^2(t) \rangle$ changes less than 10 % for $t > \tau_T$. Figure 4 exhibits m_p as a function of T_F for $\phi = 0.62, 0.64, 0.65, 0.66, 0.68$ and 0.70 with $T_1 = 2.0 \times 10^{-3}$. As we have noted, m_p is a constant for lower densities and is proportional to T_F for higher densities. It is notable that m_p behaves as a power-law function of T_F around $\phi = 0.65$ [8].

The similar critical behavior can be observed for the pressure at the final temperature T_F

$$p = \frac{1}{3L^3} \left\langle \sum_i \sum_{j>i} r_{ij} f(r_{ij}) \right\rangle + \frac{1}{3L^3} \left\langle \sum_{i=1}^N \frac{|\mathbf{p}_i|^2}{2m} \right\rangle, \quad (3)$$

where \mathbf{p}_i is the momentum of the particle i and $f(r_{ij}) \equiv -V'_{ij}(r_{ij})$ is the potential force. Figure 5 shows the pres-

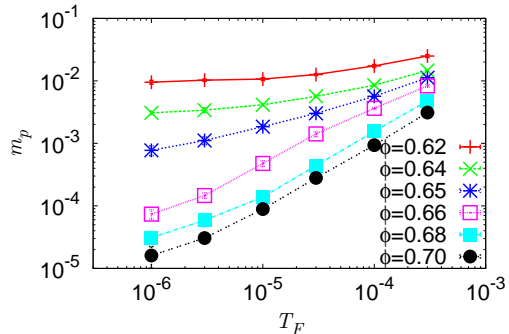


FIG. 4: (Color online) The value of plateau m_p as a function of the T_F for $T_1 = 2.0 \times 10^{-3}$ and $t_w = 10^5$ with $\phi = 0.62, 0.64, 0.65, 0.66, 0.68$, and 0.70 .

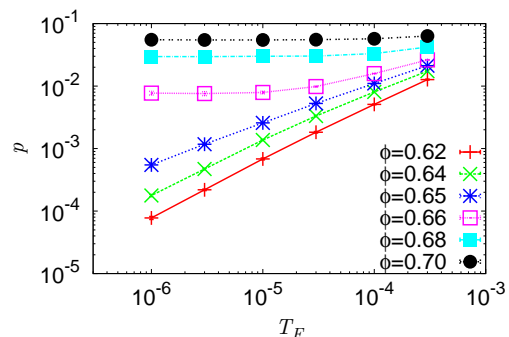


FIG. 5: (Color online) The pressure p as a function of the final temperature T_F for $T_1 = 2.0 \times 10^{-3}$ and $t_w = 10^5$ with $\phi = 0.62, 0.64, 0.65, 0.66, 0.68$, and 0.70 .

sure p as a function of T_F for $T_1 = 2.0 \times 10^{-3}$. For $\phi = 0.62$, p is almost proportional to T_F which is one of characteristic behavior of hard sphere liquids. On the other hand, p is a constant at higher volume fraction such as $\phi = 0.70$, because the pressure is determined by the rigidity of contact network of particles. It is reasonable that the rigidity of the network is insensitive to the temperature near $T = 0$.

IV. PROTOCOL DEPENDENT CRITICAL FRACTION

In this section, let us determine a critical fraction ϕ_J after the quench. It should be noted that ϕ_J is determined not by a simulation under a fixed volume but by a simulation by a compress or an expansion of the volume.

First, we prepare an equilibrium state of the volume fraction ϕ and the initial temperature T_1 . Second, we quench the system directly to T_F and keep the temperature by the velocity rescaling thermostat. Third, we further relax the system to the nearest potential energy

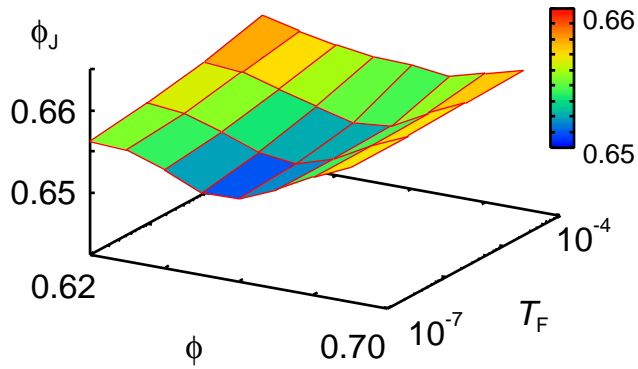


FIG. 6: (Color online) The critical fraction $\phi_J(\phi, T_F, T_I)$ as a function of ϕ and T_F for the initial temperature $T_I = 2.0 \times 10^{-3}$.

minimum by using the conjugate gradient technique [39]. Then, if the pressure p at the potential energy minimum is higher than a threshold value P_{th} , we increase the volume per particle v by Δv . Here, in order to increase the volume v , we change the system size L and the position \mathbf{r}_i of the i -th particle as $L \times \{(v + \Delta v)/v\}^{1/3}$ and $\mathbf{r}_i \times \{(v + \Delta v)/v\}^{1/3}$, respectively. After the change of the volume, the system is relaxed to the nearest potential energy minimum. We repeat the decrease of the volume fraction or expand the volume, and relax the system to a steady state. Finally, the critical fraction ϕ_J is determined from the volume per particle v_J where the pressure becomes lower than P_{th} as $\phi_J = v_{\text{av}}/v_J$ with $v_{\text{av}} \equiv \pi \sum_{i=1}^N \sigma_i^3 / (6N)$. If the pressure at the initial minimum of the potential energy is lower than P_{th} , we decrease the volume v by Δv , relax the system, and repeat the decrease and the relaxation until the pressure exceeds P_{th} . Then, we can determine the critical fraction ϕ_J from the volume per particle v_J where the pressure exceeds P_{th} . We use $P_{\text{th}} = 10^{-5}$ and $\Delta v = 0.0005$. We have checked that the critical fraction does not change if we use $P_{\text{th}} = 10^{-6}$ and $\Delta v = 0.00005$. It is also noted that the method to determine the critical fraction is almost identical to that in the previous works [8, 9, 36].

In Fig. 6, we display the critical fraction $\phi_J(\phi, T_F, T_I)$ as a function of ϕ and T_F for $T_I = 2.0 \times 10^{-3}$. Figure 7 exhibits $\phi_J(\phi, T_F, T_I)$ as a function of the initial temperature T_I and ϕ for $T_F = 1.0 \times 10^{-4}$. These figures reveal that the critical fraction ϕ_J depends on the initial equilibrium state, i. e. T_I and ϕ , and the quenched state at T_F . We note that the existence of the initial state dependence has already numerically demonstrated in Ref. [36], but the dependence on the quenched state at T_F within our knowledge has not been discussed in any other papers.

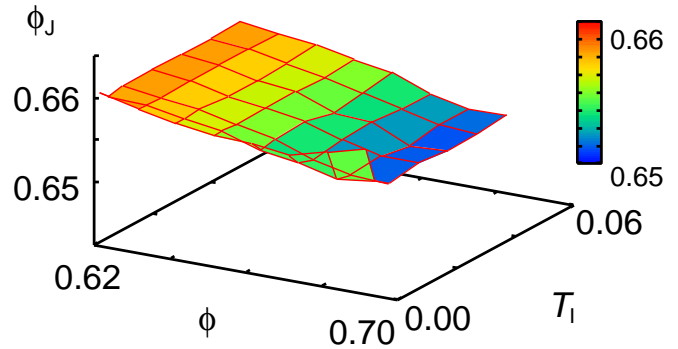


FIG. 7: (Color online) The critical fraction $\phi_J(\phi, T_F, T_I)$ as a function of T_I and ϕ for $T_F = 2.0 \times 10^{-3}$.

V. CRITICAL SCALINGS OF THE VALUE OF PLATEAU AND THE PRESSURE

In this section, let us develop the scaling analysis to characterize the behavior of MSD and the pressure. This section consists of three parts. In the first part, we summarize some asymptotic relations in the scaling functions. In the second part, we briefly introduce the method to evaluate the scaling exponents. In the last part, we discuss the values of the critical exponents.

Through our simulation, we have confirmed that the value of plateau $m_p(\phi, T_F, T_I)$ and the pressure $p(\phi, T_F, T_I)$ satisfy the scaling laws with the protocol dependent critical fraction $\phi_J(\phi, T_F, \phi)$:

$$m_p(\phi, T_F, T_I) = T_F^{a_m} \mathbf{M} \left(\frac{\phi - \phi_J(\phi, T_F, T_I)}{T_F^b} \right), \quad (4)$$

$$p(\phi, T_F, T_I) = T_F^{a_p} \mathbf{P} \left(\frac{\phi - \phi_J(\phi, T_F, T_I)}{T_F^b} \right), \quad (5)$$

where a_m , a_p , and b are the critical exponents. Here, we assume that the scaling functions $\mathbf{M}(x)$ and $\mathbf{P}(x)$ satisfy

$$\lim_{x \rightarrow \infty} \mathbf{M}(x) \propto x^{(a_m - 1)/b}, \quad (6)$$

$$\lim_{x \rightarrow -\infty} \mathbf{M}(x) \propto |x|^{a_m/b}, \quad (7)$$

$$\lim_{x \rightarrow \infty} \mathbf{P}(x) \propto x^{a_p/b}, \quad (8)$$

$$\lim_{x \rightarrow -\infty} \mathbf{P}(x) \propto |x|^{(a_p - 1)/b}, \quad (9)$$

because of the relations

$$\lim_{T_F \rightarrow 0} m_p = F_1(\phi - \phi_J), \quad (10)$$

$$\lim_{T_F \rightarrow 0} p = T_F F_2(\phi - \phi_J), \quad (11)$$

for $\phi < \phi_J$, and

$$\lim_{T_F \rightarrow 0} m_p = T_F F_3(\phi - \phi_J), \quad (12)$$

$$\lim_{T_F \rightarrow 0} p = F_4(\phi - \phi_J), \quad (13)$$

for $\phi > \phi_J$, where F_1, F_2, F_3 , and F_4 are functions depending only on $\phi - \phi_J$. The corresponding scaling forms have already discussed in terms of the replica theory [32, 33]. The similar critical scaling laws are also found for the jamming transition for sheared frictionless particles [12–19].

Figures 8 and 9 show the scaling plots based on Eqs. (4) and (5) for $T_I = 2.0 \times 10^{-3}$ and 5.0×10^{-2} , respectively. These figures confirm the validity of Eqs. (4) and (5). Here, we numerically estimate

$$a_m = 0.722 \pm 0.004, \quad a_p = 0.506 \pm 0.004, \quad b = 0.471 \pm 0.004 \quad (14)$$

for different initial temperatures $T_I = 2.0 \times 10^{-3}, 5.0 \times 10^{-3}, 1.0 \times 10^{-2}, 2.0 \times 10^{-2}, 3.0 \times 10^{-2}, 4.0 \times 10^{-2}$, and 4.0×10^{-2} by using the Levenberg-Marquardt algorithm [39], where we expand the functional forms of the scaling functions as

$$M^{-1}(x) = \begin{cases} \sum_{n=0}^5 A_n \log(x)^n & (x \geq 1), \\ \sum_{n=0}^5 B_n \log(x)^n & (x < 1), \end{cases} \quad (15)$$

$$P^{-1}(x) = \begin{cases} \sum_{n=0}^5 C_n \log(x)^n & (x \geq 1), \\ \sum_{n=0}^5 D_n \log(x)^n & (x < 1), \end{cases} \quad (16)$$

with fitting parameters A_n, B_n, C_n , and D_n . Here, we estimate the values of the fitting parameters as $(A_0, A_1, A_2, A_3, A_4, A_5) = (1.3, -5.2, 4.0, -6.2, 2.6, -0.8)$, $(B_0, B_1, B_2, B_3, B_4, B_5) = (2.2, 5.2, 16, -74, -167, -113)$, $(C_0, C_1, C_2, C_3, C_4, C_5) = (-0.9, -8.0, -12, 19, -11, 4.1)$, $(D_0, D_1, D_2, D_3, D_4, D_5) = (-1.2, 0.4, -32, -42, -36, -5.8)$. This method has been used to estimate the critical exponents for the jamming transition for sheared frictionless particles [40] and for sheared frictional grains [22]. As shown in Figs. 8 and 9, m_p and p for different initial temperature T_I satisfy the critical scalings with the same critical exponents. This indicates that the critical exponents are independent of the protocol although the critical fraction depends on it as demonstrated in the previous section.

Now, let us estimate the critical exponents in Eqs. (4) and (5) by using the previous phenomenological results on the jammed soft particles without temperature [8, 9], and the unjammed hard spheres [34, 41]. From Eqs. (4)–(9), we readily obtain

$$\lim_{T_F \rightarrow 0} m_p \propto |\phi - \phi_J|^{a_m/b}, \quad (17)$$

$$\lim_{T_F \rightarrow 0} p \propto T_F |\phi - \phi_J|^{(a_p-1)/b}, \quad (18)$$

for $\phi < \phi_J$, and

$$\lim_{T_F \rightarrow 0} m_p \propto T_F |\phi - \phi_J|^{(a_m-1)/b}, \quad (19)$$

$$\lim_{T_F \rightarrow 0} p \propto |\phi - \phi_J|^{a_p/b}, \quad (20)$$

for $\phi > \phi_J$.

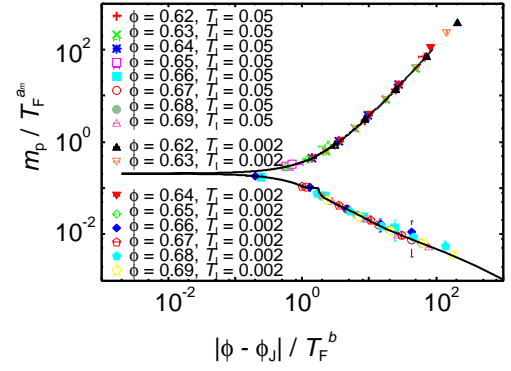


FIG. 8: (Color online) Scaling plots of m_p characterized by Eq. (4) for $T_I = 2.0 \times 10^{-3}$ and 5.0×10^{-2} with $t_w = 10^5$ and $\phi = 0.62, 0.63, 0.64, 0.65, 0.66, 0.67, 0.68$, and 0.69 . The solid line is the scaling function given by Eq. (15) with the exponents estimated as Eq. (14). The values of the other fitting parameters are shown in the text.

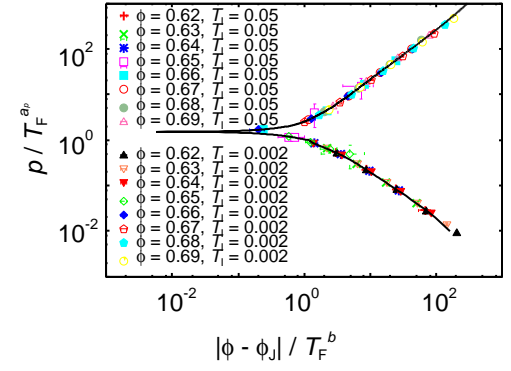


FIG. 9: (Color online) Scaling plots of p characterized by Eq. (5) for $T_I = 2.0 \times 10^{-3}$ and 5.0×10^{-2} with $t_w = 10^5$ and $\phi = 0.62, 0.63, 0.64, 0.65, 0.66, 0.67, 0.68$, and 0.69 . The solid lines are the scaling function given by Eq. (15) with the exponents Eq. (14). The values of the other fitting parameters are shown in the text.

For $\phi < \phi_J$, the pressure may satisfy

$$p \propto T_F |\phi - \phi_J|^{-1} \quad (21)$$

as suggested by the free volume theory for hard sphere liquids [41]. From the comparison of this equation with Eq. (18), we obtain

$$\frac{a_p - 1}{b} = -1. \quad (22)$$

For $\phi > \phi_J$, the pressure might be given by [8, 9]

$$p \propto |\phi - \phi_J|. \quad (23)$$

From Eqs. (20) and (23), we obtain

$$\frac{a_p}{b} = 1. \quad (24)$$

For $\phi < \phi_J$, MSD for hard sphere liquids is expected to satisfy [34]

$$m_p \sim |\phi - \phi_J|^{3/2}. \quad (25)$$

Thus, from Eqs. (17) and (25), we obtain

$$\frac{a_m}{b} = \frac{3}{2}. \quad (26)$$

From Eqs. (22), (24), and (26), we obtain the critical exponents

$$a_m = \frac{3}{4}, \quad a_p = b = \frac{1}{2}, \quad (27)$$

which are not far from the numerical estimated exponents presented in Eq. (14).

VI. DISCUSSION AND CONCLUSION

Now, let us discuss and conclude our results. First, we discuss the relationship between our approach and the papers by Berthier and Witten [29, 30]. Second, we compare our results with the prediction by the replica theory [33]. Third, we comment on the possibility to extend our model to another model of contact. In final, we summarize our results.

The previous papers [29, 30] demonstrate that the structural relaxation time satisfies a scaling relation around $\phi_G = 0.635$. We could also reproduce their scaling in our simulation, though the results are not reported in this paper. The scaling relation means that the time to escape from the plateau of $\langle r^2(t) \rangle$ for hard sphere liquids diverges at ϕ_G , but the value of plateau does not exhibit any criticality around ϕ_G because the particles can move in the cage even at ϕ_G . Moreover, the pressure continuously changes around ϕ_G because the divergence of the relaxation time is not related to the pressure. Hence, ϕ_G does not appear in the scaling relations (4) and (5). From Eq. (4), m_p for hard sphere liquids becomes zero at ϕ_J , which indicates that the dynamics of the particles in the cage is frozen at ϕ_J [34].

In Ref. [33], the replica analysis is used for the explanation of the jamming transition on the temperature-density plane for harmonic spheres. They derived the identical scaling relation (5) for the pressure with the critical exponents $a_p = b = 1/2$ corresponding to Eq. (27) and our numerical results in Eq. (14). In addition, they suggested a critical relation

$$A^* = T^\gamma A' \left(\frac{\phi - \phi_J}{T^\nu} \right) \quad (28)$$

for the optimal cage size A^* with critical exponents $\gamma = \nu = 1/2$. Because both of A^* and m_p are the characteristic length, it may be reasonable that they satisfy the

identical critical scaling if we assume that there exists only one characteristic length scale, but the values of the critical exponents $\gamma = \nu = 1/2$ from the replica theory differ from those for m_p in Eq. (14).

In this paper, we only consider the system with Hookean soft-core repulsion given by Eq. (1). For a system with the interaction potential

$$V(r_{ij}) = (1 - r_{ij}/\sigma_{ij})^{\Delta+1} \theta(\sigma_{ij} - r_{ij}) \quad (29)$$

with a exponent Δ , the scaling of the pressure given by Eq. (23) is expected to be changed as [8, 9]

$$p \propto |\phi - \phi_J|^\Delta, \quad (30)$$

which leads to

$$\frac{a_p}{b} = \Delta. \quad (31)$$

From Eqs. (22), (26), and (31), the critical exponents for the system with the potential given by Eq. (29) are expected to be

$$a_m = \frac{3}{2\Delta + 2}, \quad a_p = \frac{\Delta}{\Delta + 1}, \quad b = \frac{1}{\Delta + 1}. \quad (32)$$

The similar dependence of the critical exponents is confirmed in the sheared granular systems [18].

In conclusion, we have numerically investigated critical behavior of VP of MSD and the pressure for soft repulsive particles after quench near the jamming transition point. We verify the existence of the critical scaling relations (4) and (5), and numerically evaluate the critical exponents and the critical fraction. The critical fraction exhibits the protocol dependence, while the critical exponents are independent of the protocol, which are close to the estimation Eq. (27) in terms of the combination of the existing arguments.

Acknowledgments

We thank G. Szamel, S. Teitel, K. Miyazaki and L. Berthier for valuable discussions. This work is partially supported by the Ministry of Education, Culture, Science and Technology (MEXT), Japan (Grant Nos. 21540384 and 22740260) and the Grant-in-Aid for the global COE program "The Next Generation of Physics, Spun from Universality and Emergence" from MEXT, Japan. The numerical calculations were carried out on Altix3700 BX2 at the Yukawa Institute for Theoretical Physics (YITP), Kyoto University.

-
- [1] A. J. Liu and S. R. Nagel, *Nature* **396**, 21 (1998).
- [2] M. D. Ediger, C. A. Angell, and S. R. Nagel, *J. Phys. Chem.* **100**, 13200 (1996).
- [3] C. A. Angell, K. L. Ngai, G. B. McKenna, P. F. McMillan, and S. W. Martin, *J. Appl. Phys.* **88**, 3113 (2000).
- [4] P. G. Debenedetti and F. H. Stillinger, *Nature* **410**, 259 (2001).
- [5] H. M. Jaeger, S. R. Nagel, and R. P. Behringer, *Rev. Mod. Phys.* **68**, 1259 (1996).
- [6] D. J. Durian and D. A. Weitz, "Foams," in *Kirk-Othmer Encyclopedia of Chemical Technology*, 4th ed., edited by J. I. Kroschwitz (Wiley, New York, 1994), Vol. 11, p. 783.
- [7] P. N. Pusey, in *Liquids, Freezing and the Glass Transition, Part II*, Les Houches Summer School Proceedings Vol. 51, edited by J. -P. Hansen, D. Levesque, and J. Zinn-Justin (Elsevier, Amsterdam, 1991), Chap. 10.
- [8] C. S. O'Hern, S. A. Langer, A. J. Liu, and S. R. Nagel, *Phys. Rev. Lett.* **88**, 075507 (2002).
- [9] C. S. O'Hern, L. E. Silbert, A. J. Liu, and S. R. Nagel, *Phys. Rev. E* **68**, 011306 (2003).
- [10] M. Wyart, L. E. Silbert, S. R. Nagel, and T. A. Witten, *Phys. Rev. E* **72**, 051306 (2005).
- [11] T. S. Majmudar, M. Sperl, S. Luding, and R. P. Behringer, *Phys. Rev. Lett.* **98**, 058001 (2007).
- [12] P. Olsson and S. Teitel, *Phys. Rev. Lett.* **99**, 178001 (2007).
- [13] T. Hatano, M. Otsuki, and S. Sasa, *J. Phys. Soc. Jpn.* **76**, 023001 (2007).
- [14] T. Hatano, *J. Phys. Soc. Jpn.* **77**, 123002 (2008).
- [15] B. P. Tighe, E. Woldhuis, J. J. C. Remmers, W. van Saarloos, and M. van Hecke, *Phys. Rev. Lett.* **105**, 088303 (2010).
- [16] T. Hatano, *Prog. Theor. Phys. Suppl.* **184**, 143 (2010).
- [17] M. Otsuki and H. Hayakawa, *Prog. Theor. Phys.* **121**, 647 (2009).
- [18] M. Otsuki and H. Hayakawa, *Phys. Rev. E* **80**, 011308 (2009).
- [19] M. Otsuki, H. Hayakawa, and S. Luding, *Prog. Theor. Phys. Suppl.* **184**, 110 (2010).
- [20] B. P. Tighe, *Phys. Rev. Lett.* **107**, 158303 (2011).
- [21] M. Otsuki and H. Hayakawa, *Prog. Theor. Phys. Suppl.* No. 195, 129 (2012).
- [22] M. Otsuki and H. Hayakawa, *Phys. Rev. E* **83**, 051301 (2011).
- [23] D. Bi, J. Zhang, B. Chakraborty and R. Behringer, *Nature* **480**, 355 (2011).
- [24] Z. Cheng, J. Zhu, P. M. Chaikin, S. E. Phan, and W. B. Russel, *Phys. Rev. E* **65**, 041405 (2002).
- [25] K. S. Schweizer, *J. Chem. Phys.*, **127**, 164506 (2007).
- [26] G. Brambilla, D. El Masri, M. Pierno, L. Berthier, L. Cipelletti, G. Petekidis, and A. B. Schofield, *Phys. Rev. Lett.* **102**, 085703 (2009).
- [27] G. Parisi and F. Zamponi, *J. Chem. Phys.* **123** 144501 (2005).
- [28] F. Krzakala and J. Kurchan, *Phys. Rev. E* **76**, 021122 (2007).
- [29] L. Berthier and T. A. Witten, *Europhys. Lett.* **86**, 10001 (2009).
- [30] L. Berthier and T. A. Witten, *Phys. Rev. E.* **80**, 021502 (2009).
- [31] A. Ikeda, L. Berthier, and P. Sollich, *Phys Rev Lett.* **109** 018301 (2012).
- [32] H. Jacquin, L. Berthier, and F. Zamponi, *Phys. Rev. Lett.* **106**, 135702 (2011).
- [33] L. Berthier, H. Jacquin, and F. Zamponi, *Phys. Rev. E* **84**, 051103 (2011).
- [34] C. Brito and M. Wyart, *J. Chem. Phys.* **131**, 024504 (2009).
- [35] Z. Zhang, et al., *Nature* **459**, 230 (2009).
- [36] P. Chaudhuri, L. Berthier, and S. Sastry, *Phys. Rev. Lett.* **104**, 165701 (2010).
- [37] D. Vågberg, P. Olsson, and S. Teitel *Phys. Rev. E* **83**, 031307 (2011).
- [38] W. Kob and J-L. Barrat, *Phys. Rev. Lett.* **78**, 4581 (1997).
- [39] W. H. Press, S. A. Teukolsky, W. T. Vetterling, and B. P. Flannery *Numerical Recipes*, 3rd ed., (Cambridge University Press, Cambridge, 2007).
- [40] P. Olsson and S. Teitel, *Phys. Rev. E* **83**, 030302(R) (2011).
- [41] Z. W. Salsburg and W. W. Wood, *J. Chem. Phys.* **37**, 798 (1962).